18

Assessing Near-Surface Soil Moisture Assimilation Impacts on Modeled Root-Zone Moisture for an Australian Agricultural Landscape

R. C. Pipunic,[1] D. Ryu,[1] and J. P. Walker[2]

18.1. INTRODUCTION

Soil moisture content is an important component of the hydrologic cycle, particularly over vegetation root-zone depths where its variation is linked to the relative fractions of evaporative and sensible heat flux (L_E and H) feedbacks to the lower atmosphere, surface runoff, and groundwater recharge [*Brutsaert*, 2005]. Quantifying these processes across catchments using land surface models (LSMs), therefore, depends on soil moisture state prediction. Improved characterization of root-zone soil moisture quantities has the potential to contribute toward better predictions for a range of hydrological processes — information that will ultimately benefit agricultural and land-use management decisions (e.g., better irrigation scheduling), numerical weather prediction (NWP; e.g., through improved L_E and H feedbacks), and emergency management (e.g., improved flood prediction). While an imperfect model structure means that improving certain model variables will not necessarily lead to improvements in predictions of all other model variables [*Drusch*, 2007], improved root-zone soil moisture can translate to improvement in predictions of other water-balance-related quantities [*Pipunic et al.*, 2013]. Therefore, the ability to routinely improve root-zone moisture prediction is an important aim, and the impact on other hydrologic variables of interest may contribute to a better understanding of model structural inaccuracies.

Inherent LSM uncertainty, resulting from errors in input data (meteorological forcing and parameter information on soil and vegetation properties) and model structural inaccuracies, is the impetus for data assimilation techniques such as the ensemble Kalman filter [EnKF: *Evensen*, 1994], where observed information is used to sequentially update/correct LSM states through time, based on both modeled and observed error statistics. For routine constraint of root-zone soil moisture prediction across catchments, assimilating relevant remotely sensed data is ideal given their broad spatial coverage at regular repeat intervals.

Brightness temperature observations from passive microwave remote sensors have proven particularly suitable for deriving spatial estimates of soil moisture [*Kerr et al.*, 2010; *Njoku et al.*, 2003]. However, these estimates have major limitations, including coarse spatial resolution (>10 km) and shallow sensing depth, which varies depending on a sensor's spectral frequency and the near-surface moisture conditions but is typically within the top few centimeters of soil at most. Therefore, the impact from assimilating such data products must be able to adequately translate to the model's deeper layers in order to improve root-zone estimates. A number of studies using synthetic data or in situ field data have shown near-surface moisture assimilation can improve root-zone predictions [e.g., *Pipunic et al.*, 2013; *Kumar et al.*, 2009; *Pipunic et al.*, 2008; *Walker et al.*, 2001; *Entekhabi et al.*, 1994], with some modest improvements to deeper soil moisture from assimilating remotely sensed near-surface moisture shown by *Reichle et al.* [2007]. More recent work demonstrating the value of assimilating remotely sensed near-surface moisture for

[1] *Department of Infrastructure Engineering, University of Melbourne, Parkville, Victoria, Australia*

[2] *Department of Civil Engineering, Monash University, Clayton, Victoria, Australia*

Remote Sensing of the Terrestrial Water Cycle, Geophysical Monograph 206. First Edition. Edited by Venkat Lakshmi.

deeper LSM moisture state predictions includes *Draper et al*. [2012] and *Liu et al*. [2011].

Remotely sensed data assimilation in a spatially distributed modeling framework generally involves greater uncertainty than is the case with more controlled scenarios using synthetic or one-dimensional field-based data. This is partly due to varying spatial scales of different data sets used for model input in addition to their measurement error, while the uncertainty in assimilated remotely sensed data may also be high [*Reichle et al*., 2007]. Furthermore, the coverage of well-calibrated independent in situ data is relatively sparse for many landscapes, posing a problem for validation on a global scale. Consequently, the availability of such data should be taken advantage of to support research that can contribute to a clearer understanding of the benefits and limitations of remotely sensed near-surface soil moisture assimilation in terms of optimizing deeper root-zone moisture predictions.

This study utilizes in situ soil moisture profile data from the OzNet monitoring network in southeastern Australia [*Smith et al*., 2012] to validate LSM assimilation results. The impact from assimilating a near-surface soil moisture data product — derived from the Advanced Microwave Scanning Radiometer for the Earth Observing System (AMSR-E) observations of the top ~1–2 cm of soil — on deeper soil moisture profile predictions from the Community Atmosphere Biosphere Land Exchange model [CABLE; *Kowalczyk et al*., 2006] is examined. CABLE is the land surface component coupled with the Met Office unified model as part of ACCESS 1.3 (Australian Community Climate and Earth-System Simulator) used for climate simulations [*Kowalczyk et al*., 2013] and is also planned for use in Australia's NWP in the near future [*Law et al*., 2012]. It has yet to be rigorously tested with the assimilation of remotely sensed data for improving moisture prediction. A $100 \times 100\,km^2$ agricultural landscape in the Yanco region of New South Wales, Australia, is the focus of the experiment, where predicted moisture states were validated against 0–5 cm, 0–30 cm, and 0–60 cm in situ moisture data from 12 OzNet sites. The aim was to show if assimilating the near-surface moisture product demonstrated potential as a dependable way to improve CABLE root-zone moisture prediction for this environment. Knowledge gained here from assimilating AMSR-E data is also assumed relevant to use of data from the successor sensor AMSR-2 [*Imaoka et al*., 2010].

The EnKF algorithm was used to update the prognostic soil moisture and temperature states for each of CABLE's six soil layers. Two specific procedures were followed here in implementing the EnKF, which can potentially remedy some common issues, but which do not appear to have been thoroughly tested in real-world applications. First, we perturbed model parameter values for key soil hydraulic properties determined from field-sampled soil [*McKenzie et al*., 2000], where perturbation was guided by the associated error information supplied in the form of 5th and 95th percentile values. Perturbing time-invariant parameters ensures the LSM state ensemble spread is maintained and avoids potential problems with ensemble collapse that will render the filter ineffective. By using parameters with error estimates determined from analysis of real field samples, this approach for generating ensembles and maintaining their spread has a sound basis when compared to directly perturbing state predictions at each time step or applying covariance inflation [e.g., *Anderson and Anderson*, 1999] prior to state updating, using values estimated through trial and error. Second, the bias correction scheme of *Ryu et al*. [2009] was implemented to remove state ensemble biases caused by nonlinear model physics. This is the first implementation of this technique in a real remotely sensed data assimilation application.

18.2. DATA SETS AND EXPERIMENTAL SETUP

The $100 \times 100\,km^2$ study area for this assimilation experiment incorporates 12 OzNet soil moisture monitoring sites in the Yanco region within the Murrumbidgee catchment [*Smith et al*., 2012]. This mostly agricultural region is dominated by crops/pasture and located in the southeast of Australia within the Murray-Darling Basin. CABLE simulations were run at 5 km spatial resolution over the area while the AMSR-E soil moisture product used for assimilation [*Owe et al*., 2008] was provided at 25 km resolution (Figure 18.1).

18.2.1. Model Specifications

The CABLE model version 2.0 was used for this research. This model calculates water and energy exchanges at the land surface for both soil and vegetation surfaces, with detailed descriptions of the model physics provided by *Kowalczyk et al*. [2006]. The soil scheme consists of a six layer soil profile over 4.60 m with layer thicknesses of: 2.2, 5.8, 15.4, 40.9, 108.5, and 287.2 cm, respectively, from top to bottom. Vertical water movement between layers is based on the Richards equation with the relationships of *Clapp and Hornberger* [1978] for hydraulic conductivity (K) and air entry potential (ψ_{aep}). CABLE can only be assigned with the one set of soil parameter values which apply to all six layers; therefore, depth varying soil hydraulic properties are not represented.

Calculations of L_E are done separately for soil and vegetation canopy surfaces, and thus the leaf area index

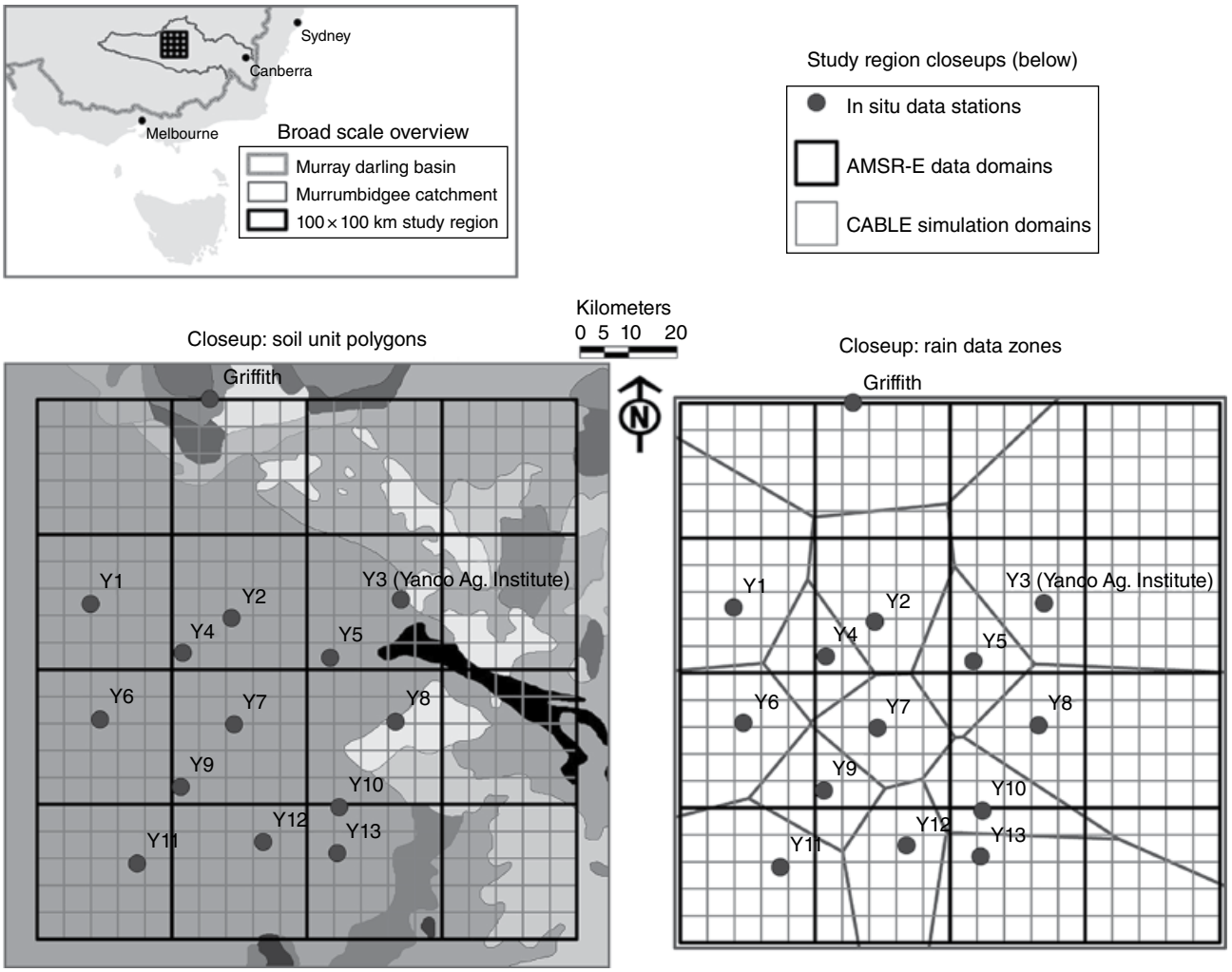

Figure 18.1 An overview of the study region location in the top left and a closeup of it in the two bottom panels. The closeups show: 25 km AMSR-E soil moisture product pixels (black squares); 5 km CABLE simulation pixels (gray squares); and locations of OzNet in situ soil moisture and rainfall stations (Y1–Y13) with Griffith meteorological station (dots). The closeup on the left shows polygons representing the mapped soil units used for prescribing model soil parameters to simulation pixels, and the closeup on the right shows the zones corresponding to in situ stations (dark gray lines), which were used to assign rainfall to simulation pixels. All other meteorological forcing from Y3 and Griffith stations were assigned to simulation pixels based on nearest proximity to either station.

(LAI) is an important model parameter for defining the fraction of bare soil to vegetation surface for energy balance calculations. A Penman-Monteith-based calculation is used for the canopy L_E, which incorporates a term linked to stomatal conductance and hence a water availability term, which consists of the available moisture content in the soil layers weighted by the relative fraction of roots in each. Vegetation root fractions for each soil layer are user-specified parameters, which are constant through the simulation time. The soil component of L_E is calculated based on the potential evaporation weighted by moisture availability in the top soil layer.

18.2.2. Model Inputs

Meteorologic forcing data determines the CABLE time step interval and simulation period, and the essential variables include short- and long-wave incoming radiation, air temperature, rainfall, wind speed, and specific humidity. Referring to Figure 18.1, forcing data is available for the Griffith and Yanco Agricultural Institute (station Y3) sites, while rainfall data is also available for each of the soil moisture stations (Y1–Y13). All of these data were used in this study and are provided on a 30 min time series, which is the integration time step for the simulations performed.

Some of the key soil parameters relevant to CABLE include wilting point (θ_{wilt}), field capacity (θ_{fc}), bulk density (ρ_{soil}), and hydraulic conductivity at saturation (K_s). Values for these used in this study are from *McKenzie et al*. [2000] and are based on field sample analysis associated with mapped spatial soil units from the Atlas of Australian Soils [*Northcote et al*., 1960–1968; see Figure 18.1] and soil type interpretations from *Northcote* [1979]. Each mapped soil unit is associated with A-horizon and B-horizon property data for at least one Dominant Principle Profile Form and possibly one or more Subdominant Principle Profile Forms. In this study the A-horizon data was used since the focus is on a generally low vegetation region including large areas of grassland with vegetation rooting depth assumed to be predominantly shallow (~0.5–1.0 m). For each spatial soil unit only the Dominant Principle Profile Form data was used.

McKenzie et al. [2000] relied on the work of *Williams et al*. [1992] for determining parameters θ_{fc} (defined as soil moisture content at 0.1 bar pressure head) and θ_{wilt} (defined as soil moisture content at 15 bar pressure head), where *Williams et al*. [1992] demonstrated pedotransfer functions for predicting the *Campbell* [1974] water retention curve using basic soil characteristic information obtainable from field samples including ρ_{soil}, soil texture, and soil structure classifications (for which they provide details). *McKenzie et al*. [2000] references a range of work conducted by CSIRO Land and Water and some published data sets as providing the basis for the K_s estimates they provide.

In summary, the key soil parameter values from *McKenzie et al*. [2000] associated with soil units in Figure 18.1 are ρ_{soil}, θ_{wilt}, θ_{fc}, and K_s. For all of these except K_s, the 5th, 50th, and 95th percentile values were included, and the 50th percentile values used for the spin-up and open loop (OL). Other key soil parameters for CABLE — θ_{sat} (soil moisture content at saturation), ψ_{aep}, and the b parameter from *Campbell* [1974] equations — were calculated using the data from *McKenzie et al*. [2000]. The θ_{sat} calculation was done using *Williams et al*. [1992]

$$\theta_{sat} = \left[1 - (\rho_{soil} / 2650)\right] \times 0.93, \tag{18.1}$$

where 2650 kg/m^3 is a standard value for density of mineral solids. Values for ψ_{aep} and b were generated from θ_{fc}, θ_{wilt}, and θ_{sat} using [*Campbell*, 1974]

$$\psi = \psi_{aep} (\theta / \theta_{sat})^{-b}, \tag{18.2}$$

where ψ is the pressure head (m) for a soil with moisture content θ, and θ_{fc} in this data set corresponds to $\psi = 1$ m and θ_{wilt} to $\psi = 150$ m. Hence there is a value for θ_{sat} and two unique values of ψ corresponding to θ_{fc} and θ_{wilt}, which enables the use of two simultaneous equations to solve for the two unknowns ψ_{aep} and b. For the key vegetation parameter LAI, the remotely sensed Moderate Resolution Imaging Spectroradiometer (MODIS) data product MYD15A2 (*Aqua*) LAI/fPAR (fraction of photosynthetically active radiation) was used (courtesy of NASA Land Processes Distributed Active Archive Center; LP DAAC), which is an 8 day composite of 1 km spatial resolution data.

Generating spatially distributed inputs from the forcing and sourced parameter data for running CABLE over the study region involved assigning the data to the 5 km simulation pixels. For point scale data, the study region was subdivided using Theissen polygons and values assigned to pixels based on the point site in nearest proximity. Thus the region was split into two for assigning all measured meteorological forcing variables (except rainfall) from the Griffith and Y3 station sites, while 14 subdivided zones were used to assign rainfall data from all soil moisture stations (Y1–Y13) including the Griffith site (see Figure 18.1).

The 1 km scale MODIS-based LAI data were spatially averaged within each 5 km simulation pixel domain. Key soil parameter data based on the work of *McKenzie et al*. [2000], and associated with the soil units in Figure 18.1, were assigned to pixels according to the dominant fraction of the soil unit polygons within each pixel. All CABLE vegetation parameters other than LAI, and soil parameters other than those previously discussed, were assigned the default global values provided with the CABLE code.

18.2.3. Assimilation Data

The AMSR-E near-surface soil moisture data used for this study was the version 04 level 3A product, on a ~25 × 25 km resolution grid, derived using the Land Parameter Retrieval Model (LPRM) developed jointly by the Vrije Universiteit Amsterdam and NASA [VUA-NASA; *Owe et al*., 2008]. *Crow et al*. [2010] found that this algorithm produced good-quality soil moisture data relative to other algorithms in a global evaluation. The data represents moisture in only the top ~1–2 cm of soil, and its availability corresponds to two repeat satellite overpasses per day at most for a geographic region — the descending overpass (~01:30–02:00 local time) and ascending overpass (~13:30–14:00 local time). Previous work [*Su et al*., 2013; *Draper et al*., 2009b] indicates that data from the descending (local morning) overpass provides superior moisture estimates for a similar region in the Murrumbidgee catchment to that focused on in this study. Hence assimilation of AMSR-E near-surface soil moisture was performed only once per day (subject to data availability) for 1:30 A.M. local time.

18.2.4. Assimilation Algorithm

The EnKF after *Evensen* [1994] is one variant of filters based on the original Kalman filter [*Kalman*, 1960] and was used for assimilation in this study. The general form of the Kalman filter can be represented as

$$\mathbf{X}_k^a = \mathbf{X}_k^f + \mathbf{K}(\mathbf{Z}_k - \mathbf{Z}_k^f), \tag{18.3}$$

where the model state vector **X** consists of 12 state values in this experiment—soil moisture and soil temperature for the six CABLE soil layers—and the observation, **Z**, is the AMSR-E soil moisture value. Subscript k refers to the assimilation time step, superscript f denotes model predicted values, and superscript a denotes analyzed (updated) values. Thus the innovation here $(\mathbf{Z}_k - \mathbf{Z}_k^f)$ represents the observation-based AMSR-E moisture minus the CABLE-predicted soil moisture for the top 2.2 cm thick soil layer.

The Kalman gain (**K**) depends on the relative uncertainties between model predictions and observed data, and weights the innovations to determine the degree to which predicted states $\mathbf{X}_k^f$ are adjusted. Therefore, defining model and observation error is crucially important and affects the filter performance, yet is very challenging especially for complex nonlinear models [*Crow and Reichle*, 2008]. The EnKF is a Monte Carlo approach to Kalman filtering based on generating ensembles of simulation predictions about a mean (or "true") value, and using the ensemble spreads for different predictions to calculate the error covariances required for **K**.

Factors contributing to LSM prediction error include uncertainty in model structure, input forcing, and parameter data. *Richter et al.* [2004] demonstrated the sensitivity of LSM water balance prediction to soil parameters, with the implication that soil parameter uncertainty can play a major part in overall water balance prediction error, particularly for soil moisture. The most comprehensive set of quantitative uncertainty information available was for soil hydraulic properties estimated from field data analysis. Hence, we endeavored to define model error based on observed uncertainty information from data analysis of key soil hydraulic parameters that directly affect modeled soil moisture dynamics through the Richards equation. As such, CABLE ensemble predictions were generated using soil parameter ensembles for parameters that had an associated uncertainty range—the procedure is discussed in the following section.

Since soil parameters are time invariant, the same parameter ensembles are applied to every simulation time step. Consequently, the model prediction ensembles were able to maintain a constant spread for the EnKF, thus avoiding the potential for ensemble collapse and filter divergence [*Whitaker and Hamill*, 2002]. These problems can occur for implementations where underestimates of model uncertainty (via ensemble spread) persist over time, and are further reduced with successive updates until ensembles collapse toward a single member. At this point the EnKF is ineffective since model predictions are weighted as highly certain, with their trajectory diverging from observed information [*Slater and Clark*, 2006]. If perturbing only forcing inputs such as rainfall [e.g., *Turner et al.*, 2008], time steps with no rain are typically associated with no rainfall error (hence no perturbation), which may result in an underestimated ensemble spread for state predictions. Consequently, applying state perturbation or covariance inflation [*Anderson and Anderson*, 1999] to ensure the ensemble spread correctly represents the overall model error relies largely on trial and error. The soil parameter perturbation applied in this work at least has some basis in uncertainty estimates from field data with no tuning required to maintain the ensemble spread.

Another feature of the EnKF application used for this work is the procedure to minimize unintended bias in model state ensembles during assimilation, as demonstrated by *Ryu et al.* [2009]. Essentially, for a model perturbed with zero-mean Gaussian noise as is typical for EnKF implementation, nonlinear model processes can result in biased ensemble state predictions that can lead to degraded impacts on deeper soil states. Potential problems with biased ensembles from parameter perturbation is also described in earlier work by *De Lannoy et al.* [2006]. The implemented bias correction procedure of *Ryu et al.* [2009] is discussed more in the following section.

18.3. METHODOLOGY

Eight years of data were compiled for the study region (Figure 18.1)—from 1 July 1 2002 to 30 June 2010—including meteorological forcing and parameters (with time varying LAI) at the 5 km scale, and AMSR-E moisture data at the 25 km scale for the 1:30 A.M. local time overpass. Following a 10 year spinup to provide initial soil moisture and temperature state values for all six CABLE soil layers, a single unperturbed OL simulation was run with the full 8 years of compiled input data. The first 4 years of this—1 July 2002 to 30 June 2006—were used for examining model AMSR-E bias and determining factors for correction. The following 4 years—1 July 2006 to 30 June 2010—was the main experiment period where assimilation was performed after bias correction.

There were three main components to the experimental work. First was determining and removing the systematic

bias between AMSR-E moisture data and CABLE moisture predictions for its top soil layer. Setting up the parameter error perturbation along with the online bias correction from *Ryu et al*. [2009] was then carried out for EnKF implementation. Finally, the assimilation was performed and the resulting soil moisture predictions assessed against in situ data.

18.3.1. Observed-Modeled Bias Removal

The statistical basis for data assimilation is to correct for random model errors. Therefore, systematic biases between modeled and observed states need to be accounted for and removed prior to assimilation. Rescaling remotely sensed soil moisture data to match the climatology of the model predicted near-surface moisture is somewhat standard practice [e.g., *Draper et al*., 2009a; *Drusch et al*., 2005].

A rescaling approach was applied to match the mean and standard deviation of the AMSR-E data series to that of the CABLE predicted series for the top 0–2.2 cm soil layer. A limitation to removing long-term model observation climatological differences is the relatively short record of remotely sensed data (~10 years for AMSR-E). This makes it difficult to know if the rescaling based on a certain period is representative of future differences, which has potential implications for rescaling new data as it becomes available in real-world modeling applications. To test this, the rescaling relationship between AMSR-E moisture data and CABLE was determined for an initial 4 year period, which was then applied to rescale data over the following 4 year period for use in the data assimilation experiment.

Rescaling the AMSR-E moisture series for the period 1 July 2002 to 30 June 2006 removed much of the bias relative to CABLE. Using the same mean and standard deviation as a benchmark, the rescaling was applied for the assimilation period of 1 July 2006 to 30 June 2010 for which much of the bias was also removed (Figure 18.2), and the resulting 4 year rescaled AMSR-E data series was used in the assimilation.

18.3.2. EnKF Implementation

Uncertainty in both the observed data and the model predictions forms the basis for data assimilation but remain difficult to define. Major sources of error for LSMs such as CABLE are model physics, where complex physical interactions are represented with generalized relationships; inaccurate parameters related to the water balance due to a general lack of quality and quantity (including spatial detail) of such data, errors in key meteorological forcing inputs, and, in the shorter term, uncertain initial state variables. For the EnKF to work optimally, the total model error from all of these sources needs to be adequately represented by the ensemble spread, which at present is extremely challenging.

The strategy here was perturbing key CABLE soil parameter inputs for which uncertainty information was available, resulting in a consistent ensemble spread for soil state predictions reflecting the impact of this uncertainty. State values for all six CABLE soil layers were also perturbed for the initial time step of the 1 July 2006 to 30 June 2010 assimilation period. An ensemble of random zero-mean Gaussian variates, together with the standard deviation (σ) of available uncertainty estimates, were used

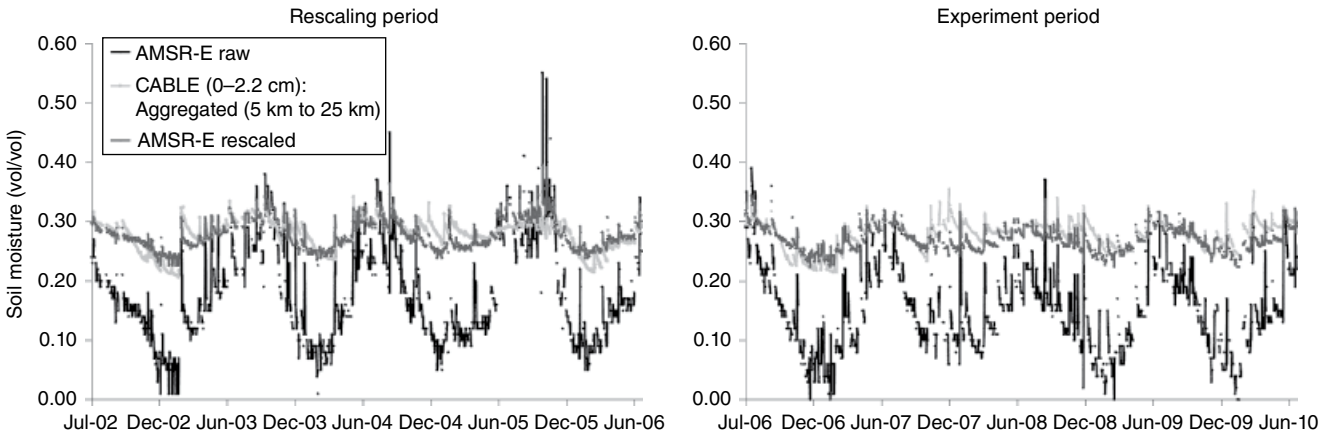

Figure 18.2 Time series plots showing bias removal between AMSR-E (local morning overpass) and CABLE soil moisture for a sample AMSR-E domain in the study region. The mean and standard deviation of CABLE predictions over the rescaling period in the left-hand plot was used to rescale the AMSR-E series. The plot on the right indicates this was adequate for removing much of the bias over the experiment period, and the resulting AMSR-E data were used for assimilation here.

to generate ensembles for the different inputs within the 95% confidence interval ($\pm 1.96\sigma$). The ensemble size used here was 30 members. Perturbation of soil parameters was performed once and the resulting parameter ensembles used throughout the whole experiment period. Care was taken to ensure ensemble member values for particular parameters were sensible in relation to corresponding members for other parameters (e.g., each perturbed θ_{fc} value, ranked from minimum to maximum, is matched with a perturbed θ_{wilt} value that is in the corresponding position of minimum to maximum rank ordered θ_{wilt} values, to avoid physically unrealistic combinations of these two parameters).

With no knowledge of the true initial state values across the study region, uncertainty estimates were made for their ensemble generation with: $\sigma = 0.04$ vol/vol for the six soil moisture states and $\sigma = 4\,°C$ for the six soil temperature states. The 5th and 95th percentile values provided with θ_{wilt}, θ_{fc}, and ρ_{soil} soil parameters sourced directly from *McKenzie et al*. [2000] were used for estimating σ values, from which ensembles were generated for each of the parameters with 95% confidence interval.

Corresponding ensemble member values for θ_{fc} and θ_{wilt} were sorted in ascending order to ensure a reasonable available water range between the two, with an assumption of some correlation between the two with changes in soil texture. Ensemble members for ρ_{soil} were used to calculate an ensemble for θ_{sat} using equation 18.1, and θ_{sat} ensemble member values were sorted in ascending order to correspond with ascending values of θ_{fc} and θ_{wilt} members. The ensembles for all these parameters were then used to calculate ensembles for ψ_{aep} and b using equation 18.2. Calculating the ensemble values for these (and θ_{sat}) ensured consistency in the relationships between corresponding ensemble members for all related parameter values.

Values for K_s are available with the *McKenzie et al*. [2000] soils map data and are classified according to a corresponding $\log_{10}$ linear scale with increments of 0.5 per class, with uncertainty information given only in terms of $\pm n$ classes. The strategy here involved generating ensembles for inputs within a 95% confidence interval, therefore $\pm n$ was treated as the bounds for this interval, and the $\log_{10}$ linear scale value for K_s associated with each soil unit was treated as the ensemble mean value (used in spinup and OL). Ensemble generation was done here with the $\log_{10}$ linear scale data assuming a Gaussian distribution, and the resulting distribution of values was transformed back to provide ensembles for K_s distributed on a $\log_{10}$ scale with units of millimeters/hour.

Observational error applied to the AMSR-E (VUA-NASA) moisture product for the assimilation was $\sigma = 0.06$ vol/vol [*Parinussa et al*., 2011]. While validation of this product by *Draper et al*. [2009b] over the Murrumbidgee catchment (where this experiment was performed) resulted in an error estimate of ~0.02–0.04 vol/vol (after rescaling the product to minimize bias relative to in situ validation data), the more conservative estimate of 0.06 vol/vol was used.

As previously discussed, a problem with the EnKF is that even when applying Gaussian perturbations for error representation, predicted state ensemble means are often biased during the assimilation due to nonlinear model processes. The approach of *Ryu et al*. [2009] used to address this involved running an additional ensemble member with no model perturbation (the OL) in parallel with the other 30 members resulting from perturbations. Prior to calculating model error covariances for **K** [equation 18.3] at each EnKF state update time step, the ensemble mean of the perturbed predictions is corrected (by correcting each perturbed ensemble member accordingly) to remove bias relative to the single unperturbed member. The bias-corrected ensemble of predictions is then used as per normal for covariance calculations, and the resulting mean of the updated state ensemble is used as the initial state value for the unperturbed (OL) member for the next prediction period between observations.

Ryu et al. [2009] describe specific soil moisture biases introduced by ensemble end members near the bounds of the model soil moisture range, defined in this study by θ_{wilt} and θ_{sat}, which are the lower and the upper bounds, respectively. In many models (including CABLE) any members less than θ_{wilt} will be reset to θ_{wilt} and any members greater than θ_{sat} are reset to θ_{sat}. Therefore, as ensemble means approach these bounds for either near dry or near saturated conditions, the normal distribution of the ensembles implies that a number of members will exceed and therefore be reset, leading to a concentration of members with boundary values. This skews the ensemble distributions and biases the means away from the boundaries. To correct for this bias, the *Ryu et al*. [2009] approach needs to adjust the skewed members toward the boundaries, which has the potential to excessively reduce the ensemble spread and lead to filter divergence. However, it was found that this problem can be avoided by perturbing model soil parameters, which ensured an adequate spread is maintained, at least in terms of uncertainty introduced by the key soil parameters.

Finally, given the spatial disparity between model simulation (5 km) and AMSR-E product (25 km) resolutions (Figure 18.1), the average of predictions for all 5 km simulation pixels within each AMSR-E footprint domain were first calculated, and the up-scaled values used to calculate innovations with the corresponding ASMR-E data [bracketed term in equation 18.3]. The resulting update terms (innovation weighted by **K**) were then applied back to the states for each individual 5 km simulation domain. This approach ensured the spatial variability of moisture between 5 km simulation pixels was maintained.

18.3.3. Assessing the Assimilation

The experimental simulation was performed for the 4 year period spanning from 1 July 2006 to 30 June 2010. The AMSR-E soil moisture data for the ~01:30 A.M. local overpass time were assimilated into the top soil layer of the CABLE LSM, and the impact on updates made to its deeper root-zone moisture state predictions was assessed for 12 OzNet station sites: Y1 – Y10, Y12, and Y13 (Figure 18.1).

Assimilation outputs for the 5 km simulation pixels were compared against available in situ data from collocated OzNet stations over the 4 year period. Moisture values for the different soil layers in CABLE, and also those measured in situ at the stations (for 0–5 cm—except for Y3 which was 0–7 cm, 0–30 cm, and 30–60 cm depths) were depth averaged where necessary to enable direct comparisons for 0–5 cm, 0–30 cm and 0–60 cm depth ranges. The calculation of depth averaged values for comparisons is summarized in Table 18.1. For this predominantly pasture/crop region the root zone is defined as 0–60 cm.

To facilitate meaningful/bias-free error assessment of assimilation results, the in situ observed data series for each validation site were rescaled (by matching their series mean and standard deviation) to the OL series for the experiment period. This is consistent with the assimilation performed relative to the CABLE OL climatology (using rescaled AMSR-E data). Metrics used to compare both OL and assimilation/updated (UP) outputs with rescaled in situ data were the root-mean-squared error (RMSE) and the coefficient of determination (R^2).

The overall impact over the study region was assessed for the three soil depths, where mean differences between UP and OL in terms of both RMSE and R^2 values were calculated across the 12 sites. A permutation test (with 10,000 resamples) was applied where the statistical significance of these mean differences (indicating the significance of the overall impact from data assimilation) was tested. Therefore, the null hypothesis was that the mean differences between UP and OL across the 12 sites in terms of RMSE and R^2 values is zero. Determining the significance of any of the mean differences (therefore the significance of the overall assimilation impacts) was through p values resulting from the tests.

Normalized values for RMSE and R^2, which represent improvement or degradation from OL to UP, were also calculated and plotted to summarize the overall assimilation impacts for the three depths. The normalized RMSE is simply the ratio between the RMSE for UP and OL:

$$\mathrm{NRMSE} = \frac{\mathrm{RMSE}_{\mathrm{UP}}}{\mathrm{RMSE}_{\mathrm{OL}}}, \tag{18.4}$$

while for R^2 the ratio between the unexplained variance in UP to the unexplained variance in OL was used:

$$\mathrm{NR}^2 = \frac{\left(1 - R^2_{\mathrm{UP}}\right)}{\left(1 - R^2_{\mathrm{OL}}\right)}. \tag{18.5}$$

Values of NRMSE = 1 and $\mathrm{NR}^2 = 1$ from equations 18.4 and 18.5 indicate no impact on CABLE from the assimilation in terms of changes in residual error (RMSE) or explained variance (R^2), respectively. Values for each that are <1 indicate improvement, and values for each that are >1 represent degradation from the assimilation according to the respective metrics.

Table 18.1 Calculations applied for averaging modeled and in situ soil moisture data over different depths (in cm) to enable direct comparisons between them

	In Situ Soil Moisture	CABLE Soil Moisture
0–5 cm (0–7 cm for Y3 only)	Direct measurements	$\frac{\left(2.2\times\theta^{\mathrm{M}}_{0-2.2}\right)+\left(2.8\times\theta^{\mathrm{M}}_{2.2-8}\right)}{5}$ $\frac{\left(2.2\times\theta^{\mathrm{M}}_{0-2.2}\right)+\left(4.8\times\theta^{\mathrm{M}}_{2.2-8}\right)}{7}$
0–30 cm	Direct measurements	$\frac{\left(2.2\times\theta^{\mathrm{M}}_{0-2.2}\right)+\left(5.8\times\theta^{\mathrm{M}}_{2.2-8}\right)+\left(15.4\times\theta^{\mathrm{M}}_{8-23.4}\right)+\left(6.6\times\theta^{\mathrm{M}}_{23.4-64.3}\right)}{30}$
0–60 cm (root zone)	$\frac{\left(30\times\theta^{\mathrm{I}}_{0-30}\right)+\left(30\times\theta^{\mathrm{I}}_{30-60}\right)}{60}$	$\frac{\left(2.2\times\theta^{\mathrm{M}}_{0-2.2}\right)+\left(5.8\times\theta^{\mathrm{M}}_{2.2-8}\right)+\left(15.4\times\theta^{\mathrm{M}}_{8-23.4}\right)+\left(36.6\times\theta^{\mathrm{M}}_{23.4-64.3}\right)}{60}$

Note: Moisture content data is represented by θ, with superscripts indicating whether it is an in situ measurement (I) or model prediction (M), and subscripts indicating the depth range of the data (i.e., for CABLE they represent model soil layer depths).

18.4. RESULTS AND DISCUSSION

A complete summary of assessments for assimilation impacts over the root zone is displayed in Table 18.2, showing R^2 and RMSE metrics for both OL and UP relative to in situ data. Mean differences between OL and UP for these metrics across the 12 validation sites are also included along with corresponding p values from the permutation tests, which tested whether the mean differences are significantly different to zero as an indication of how significant the overall assimilation impacts were.

From Table 18.2, the greatest improvements in UP compared to OL were for the 0–5 cm depth, with improved RMSE and R^2 scores for 7 out of 12 and 10 out of 12 stations respectively. The 0–5 cm depth was also the only depth range where the overall improvement from assimilation across all sites was statistically significant, but only in terms of mean improvement in R^2 for which a p value of 0.009 indicates significance at the 99% confidence level. For 0–30 cm and 0–60 cm depths, there was improvement in terms of RMSE for 7 out 12 and 6 out of 12 stations, respectively, and improvement in R^2 for 8 out of 12 and 7 out of 12 stations, respectively. None of the overall changes from the assimilation across the 12 sites for 0–30 cm and 0–60 cm depths, as per average RMSE and R^2 differences, were statistically significant according to corresponding p values from permutation tests. These results demonstrate some difficulty in improving modeled soil moisture states with depth from the assimilation of a shallow moisture product. It also appears that the assimilation may be slightly better at improving the temporal variance of predictions as indicated by R^2 than reducing overall residual error as indicated by reduced RMSE.

Figure 18.3 provides a visual summary of overall improvement to soil moisture in the 3 depths across the 12 sites. It shows median and interquartile ranges of NRMSE and NR^2 [equations 18.4 and 18.5] for the 12 sites. All points in the plot fall below 1 for both NMRSE and NR^2, indicating some overall improvement based on the median values of these metrics. By contrast, the mean difference values for RMSE and R^2 in Table 18.2 indicate slight overall degradation for some depths. However, given the very small sample size of 12 stations, the means are likely to be skewed by one or two extreme differences for each depth (the validity of the permutation tests for means is based on the resampling of 10,000 sets of differences).

Plots in Figure 18.4 are time series results illustrating the assimilation impacts on the root-zone moisture prediction, sampled from three sites. One where there was

Table 18.2 Root-mean-squared error (RMSE) and coefficient of determination (R^2) assessments of predicted soil moisture from the 4 year assimilation experiment relative to in situ data for the 12 OzNet sites Y1–Y10, Y12, and Y13

	0–5 cm				0–30 cm				0–60 cm			
	RMSE		R^2		RMSE		R^2		RMSE		R^2	
Site	OL	UP	OL	UP	OL	UP	OL	UP	OL	UP	OL	UP
Y1	**0.021**	**0.018**	**0.34**	**0.63**	**0.022**	**0.018**	**0.19**	**0.53**	**0.021**	**0.019**	**0.14**	**0.36**
Y2	0.008	0.026	0.39	0.39	0.007	0.028	0.50	0.11	0.007	0.029	0.48	0.01
Y3	**0.017**	**0.012**	**0.36**	**0.66**	**0.018**	**0.014**	**0.25**	**0.46**	**0.017**	**0.014**	**0.25**	**0.44**
Y4	0.007	0.007	**0.54**	**0.63**	**0.011**	**0.009**	**0.25**	**0.40**	0.010	0.010	**0.29**	**0.33**
Y5	0.008	0.009	**0.49**	**0.65**	**0.012**	**0.011**	**0.08**	**0.38**	0.009	0.012	0.36	0.18
Y6	**0.014**	**0.011**	**0.16**	**0.43**	**0.018**	**0.014**	**0.00**	**0.11**	**0.018**	**0.015**	**0.01**	**0.04**
Y7	0.007	0.007	**0.49**	**0.59**	0.009	0.009	**0.26**	**0.43**	**0.009**	**0.008**	**0.21**	**0.45**
Y8	**0.007**	**0.006**	**0.48**	**0.58**	0.007	0.009	0.58	0.41	0.007	0.010	0.55	0.23
Y9	**0.022**	**0.016**	**0.12**	**0.32**	**0.024**	**0.020**	**0.01**	**0.05**	**0.024**	**0.020**	**4.2E-7**	**0.02**
Y10	0.006	0.011	0.57	0.37	0.007	0.011	0.42	0.38	0.007	0.010	0.46	0.45
Y12	**0.008**	**0.006**	**0.40**	**0.67**	**0.011**	**0.009**	**0.10**	**0.21**	**0.012**	**0.010**	**2.1E-3**	**0.06**
Y13	**0.008**	**0.007**	**0.33**	**0.46**	0.007	0.008	0.47	0.39	0.008	0.008	0.37	0.29
μ (mean differences)	-2.5×10^{-4}		0.14		-5.8×10^{-4}		0.06		-1.3×10^{-3}		−0.02	
p value for μ (H_0: $\mu = 0$)	0.476		0.009		0.408		0.196		0.305		0.612	

Note: Values for each metric in bold indicate an improvement from the assimilation, and the nonbold font indicates either no improvement or a degraded impact. The bottom two rows include the means of differences between OL and UP in terms of RMSE and R^2, along with corresponding p values from permutation tests for whether the mean differences significantly differ from zero.

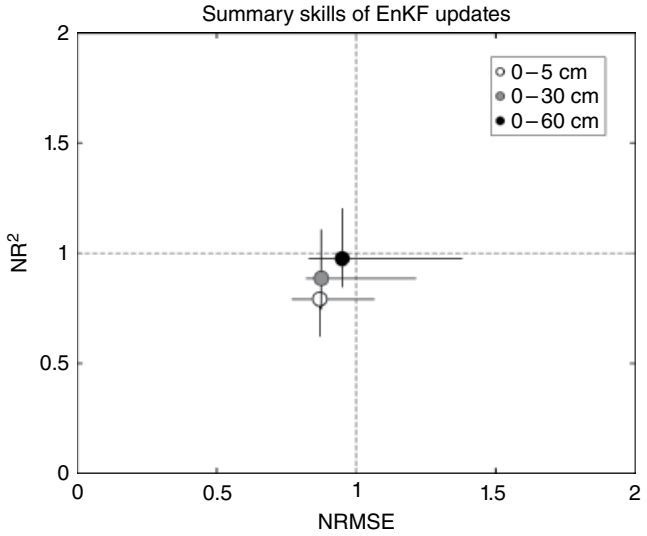

Figure 18.3 Plot showing the median NRMSE against the median NR^2 [equations 18.4 and 18.5] across the 12 validation sites for the 3 soil depths examined, along with interquartile ranges (25th and 75th percentiles). Grid lines on the plot at 1 for both NRMSE and NR^2 signify no difference between UP and OL, while values <1 signify improvement from the assimilation and values >1 signify degradation.

clear root-zone improvement according to both RMSE and R^2 (Y1), one where there was degradation (Y5), and one where there was minor improvement in either one or both metrics (Y6). The Y6 site is of particular interest as the in situ data contains information from isolated irrigation events. The root-zone time series plots shown in Figure 18.4 highlight the ability of the assimilation to translate information on AMSR-E and CABLE differences for the near-surface down to deeper root-zone states in CABLE. Another feature to note from Figure 18.4 is the ensemble extremes in each plot, which demonstrate the maintained ensemble spread over the 4 year experiment period due to the input of perturbed parameter ensembles.

For Y5, where the UP root-zone series was degraded overall from OL (Table 18.2), most of the adjustments appear to be in the right direction relative to the in situ data (except for around December 2007), but they overshoot it, which is generally the case for most other sites where the root zone has also been degraded. This may be an issue of imbalanced model-observation error representation or coupling strength between the near surface and deeper soil layers in CABLE. A more detailed investigation is necessary to better understand the degraded results.

For the Y6 series where known irrigation events are present in the in situ data (~September 2006 and 2007), there is negligible evidence of it in the modeled series. While it is expected that AMSR-E is able to detect such events relative to dry surrounds, and for such information to be assimilated into the model, in this case the irrigation was known to be at the paddock scale only (in the order of ~100s of m^2) and hence the lack of impact. This highlights a particular limitation of broad-scale (~10s of km^2) moisture data from microwave remote sensing in terms of constraining water balances and providing useful information for agricultural decisions relevant to specific small-scale areas (~100s of meters to ~1 km). Also relevant to this issue is the large-scale discrepancy between model inputs (forcing and parameters), assimilated data products, and the point scale validation data, which adds to the difficulty of defining uncertainty and evaluating results in experiments such as this.

18.5. CONCLUSIONS

Assimilating remotely sensed near-surface soil moisture into the CABLE LSM was shown to make some improvement to deeper moisture state prediction. However, the only overall improvement across all 12 validation sites that was statistically significant (at the 99% confidence level) was the average improvement in predicted variance by 0.14 over the 0–5 cm depth. The ability for improvement was also shown to drop off with increasing depth—for the full 0–60 cm root zone, some improvement was evident for only just over half of the validation sites. While a larger sample size of validation data would enable stronger conclusions to be drawn, investigating near-surface and deeper moisture state coupling in CABLE, and the sensitivity of the near-surface and deeper state error correlations to different perturbations, may also provide insight into the cause of degraded assimilation impacts.

Perturbing key soil parameters with informed uncertainty estimates successfully maintained predicted ensemble spreads for the EnKF, without applying covariance inflation or perturbations based on trial and error. Consequently, the online bias correction that was implemented worked well, with no evidence of it leading to ensemble collapse, which may be a problem in some cases when ensemble mean moisture state values approach the extremes of the model soil moisture range. The presence of small-scale irrigation in the study region explicitly highlighted the issue of uncertainty from spatial scale discrepancies between data used for model input, assimilation, and validation, particularly for agricultural areas. Therefore, information from broad-scale remotely sensed data (~10s of km) such as AMSR-E may not always provide water balance information that is useful for decision making at the farm/paddock scale.

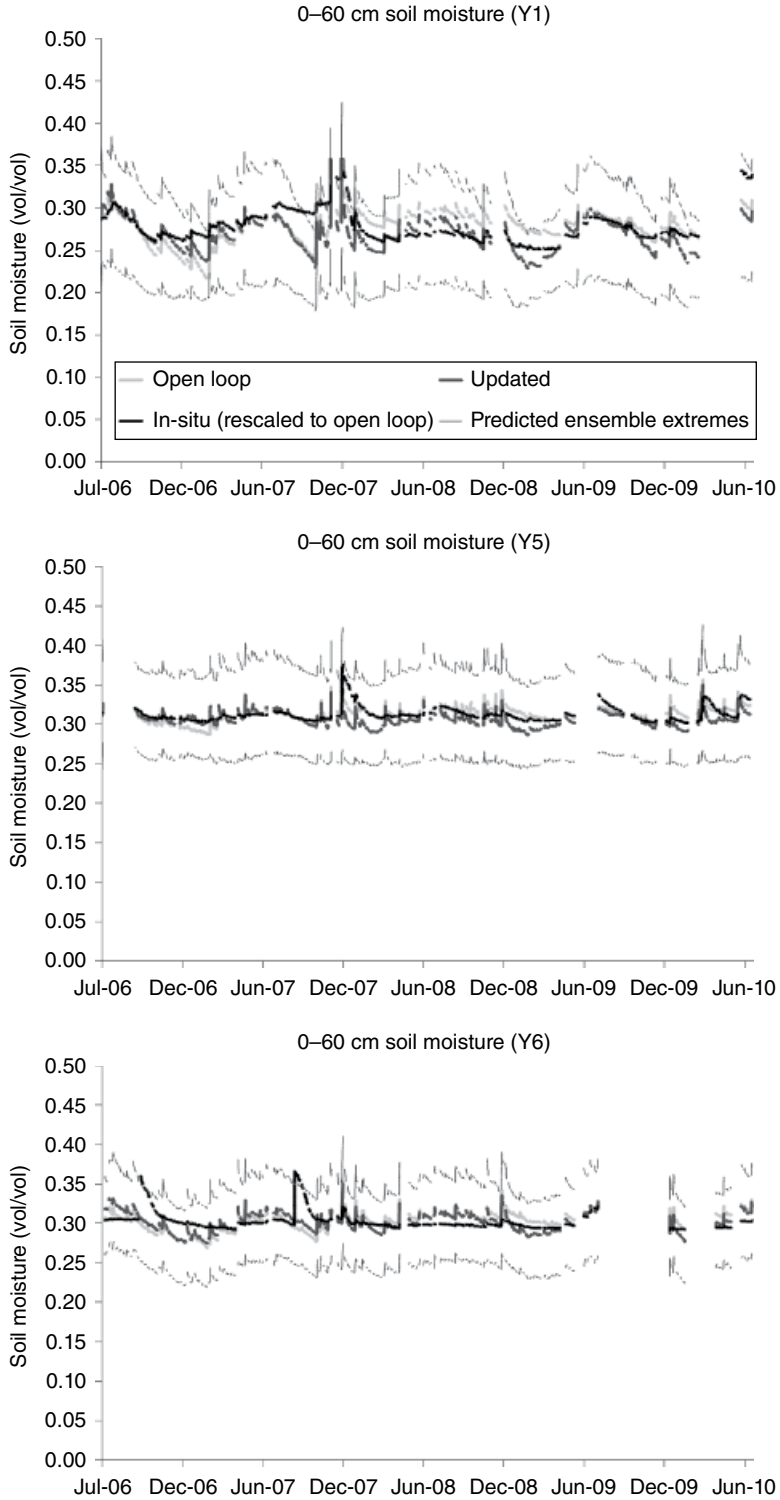

Figure 18.4 Time series plots of data sampled at 1:30 A.M. (local) time for three OzNet station sites, with a priori output from the assimilation procedure. Shown are the impacts on CABLE root-zone moisture predictions resulting from the assimilation of AMSR-E soil moisture data at previous update times, including a priori maximum and minimum ensemble end members resulting from the perturbed parameter ensemble inputs. UP for station Y1 (top) was an overall improvement on OL (see Table 18.2), for Y5 (middle) it was degraded overall, and for Y6 (bottom) there was some improvement (only in terms of RMSE). Note the impact on Y6 in situ data from irrigation in ~ September 2006 and 2007.

ACKNOWLEDGMENTS

This work was supported by the Department of Primary Industries (DPI), Victoria, Australia, and the Australian Research Council (ARC) through ARC Linkage Project LP0989441. We would also like to acknowledge the landowners in the Yanco region who allowed the OzNet stations to operate on their property. Rodger Young, field engineer at The University of Melbourne, provided valuable insights from his records and personal experience of many years work on the Yanco OzNet stations—in particular for confirming the occurrence and extent of irrigation events relevant to data sets used in this study. We also thank Lionel Siriwardena from the Department of Infrastructure of Engineering, The University of Melbourne, and Kaighin McColl from his time as research assistant at the University of Melbourne for helping to prepare the meteorological forcing data sets used in this study.

REFERENCES

Anderson, J. L., and S. L. Anderson (1999), A Monte Carlo implementation of the nonlinear filtering problem to produce ensemble assimilations and forecasts, *Monthly Weather Rev., 127*, 2741–2758.

Brutsaert, W. (2005), *Hydrology: An Introduction*, Cambridge Univ. Press, Cambridge, United Kingdom.

Campbell, G. S. (1974), A simple model for determining unsaturated conductivity from moisture retention data, *Soil Sci., 117*, 311–314.

Clapp, R. B., and G. M. Hornberger (1978), Empirical equations for some soil hydraulic properties, *Water Resourc. Res.*, *14*, 601–604.

Crow, W. T., and R. H. Reichle (2008), Comparison of adaptive filtering techniques for land surface data assimilation, *Water Resourc. Res., 44*, W08423.

Crow, W. T., D. G. Miralles, and M. H. Cosh (2010), A quasi-global evaluation system for satellite-based surface soil moisture retrievals, *IEEE Trans. Geosci. Remote Sens., 48*, 2516–2527.

De Lannoy, G. J. M., P. R. Houser, V. R. N. Pauwels, and N. E. C. Verhoest (2006), Assessment of model uncertainty for soil moisture through ensemble verification, *J. Geophys. Res., 111*, D10101.

Draper, C. S., J.-F. Mahfouf, and J. P. Walker (2009a), An EKF assimilation of AMSR-E soil moisture into the ISBA land surface scheme, *J. Geophys. Res., 114*, D20104.

Draper, C. S., J. P. Walker, P. Steinle, R. d. Jeu, and T. Holmes (2009b), An evaluation of AMSR-E derived soil moisture over Australia, *Remote Sens. Environ., 113*, 703–710.

Draper, C. S., R. H. Reichle, G. J. M. De Lannoy, and Q. Liu (2012), Assimilation of passive and active microwave soil moisture retrievals, *Geophys. Res. Lett., 39*, L04401.

Drusch, M. (2007), Initializing numerical weather prediction models with satellite-derived surface soil moisture: Data assimilation experiments with ECMWF's Integrated Forecast System and the TMI soil moisture data set, *J. Geophys. Res., 112*, D03102.

Drusch, M., E. F. Wood, and H. Gao (2005), Observation operators for the direct assimilation of TRMM microwave imager retrieved soil moisture, *Geophys. Res. Lett., 32*, L15403.

Entekhabi, D., H. Nakamura, and E. G. Njoku (1994), Solving the inverse problem for soil moisture and temperature profiles by sequential assimilation of multifrequency remotely sensed observations, *IEEE Trans. Geosci. Remote Sens., 32*, 438–448.

Evensen, G. (1994), Sequential data assimilation with a nonlinear quasi-geostrophic model using Monte Carlo methods to forecast error statistics, *J. Geophys. Res. Oceans, 99*, 10,143–10,162.

Imaoka, K., M. Kachi, M. Kasahara, N. Ito, K. Nakagawa, and T. Oki (2010), Instrument performance and calibration of AMSR-E and AMSR2, *Int. Arch. Photogram. Remote Sens. Spatial Inform. Sci., 38*, 13–16.

Kalman, R. E. (1960), A new approach to linear filtering and prediction problems, *Trans. ASME J. Basic Eng., 82*, 35–45.

Kerr, Y. H., et al. (2010), The SMOS mission: New tool for monitoring key elements of the global water cycle, *Proc. IEEE*, *98*, 666–687.

Kowalczyk, E. A., Y. P. Wang, R. M. Law, H. L. Davies, J. L. McGregor, and G. Abramowitz, (2006), The CSIRO Atmosphere Biosphere Land Exchange (CABLE) model for use in climate models and as an offline model, Paper 013, CSIRO Marine and Atmospheric Research, Aspendale, Australia.

Kowalczyk, E. A., L. Stevens, R. M. Law, M. Dix, Y. P. Wang, I. N. Harman, K. Haynes, J. Srbinovsky, B. Pak, and T. Ziehn (2013), The land surface model component of ACCESS: Description and impact on the simulated surface climatology, *Austral. Meteorol. Oceanogr. J., 63*, 65–82.

Kumar, S. V., R. H. Reichle, R. D. Koster, W. T. Crow, and C. D. Peters-Lidard, (2009), Role of subsurface physics in the assimilation of surface soil moisture observations, *J. Hydrometeorol., 10*, 1534–1547.

Law, R. M., M. R. Raupach, G. Abramowitz, I. Dharssi, V. Haverd, A. J. Pitman, L. Renzullo, A. Van Dijk, and Y.-P. Wang, (2012), The Community Atmosphere Biosphere Land Exchange (CABLE) model roadmap for 2012–2017, Tech. Rep. 057, *The Centre for Australian Weather and Climate Research (CAWCR),* Aspendale, Australia.

Liu, Q., R. H. Reichle, R. Bindlish, M. H. Cosh, W. T. Crow, R. de Jeu, G. J. M. De Lannoy, G. J. Huffman, and T. J. Jackson, (2011), The contributions of precipitation and soil moisture observations to the skill of soil moisture estimates in a land data assimilation system, *J. Hydrometeorol.*, *12*, 750–765.

McKenzie, N. J., D. W. Jacquier, L. J. Ashton, and H. P. Cresswell, (2000), Estimation of soil properties using the Atlas of Australian Soils, Tech. Rep. 11/00, CSIRO Land and Water, Canberra, Australia.

Njoku, E. G., T. J. Jackson, V. Lakshmi, T. Chan, and S. V. Nghiem (2003), Soil moisture retrieval from AMSR-E, *IEEE Trans. Geosci. Remote Sens., 41*, 215–229.

Northcote, K. H. (1979), *A Factual Key for the Recognition of Australian Soils,* 4th ed., Rellim Technical Publications, Glenside, Australia.

Northcote, K. H., et al. (1960–1968), Atlas of Australian Soils, Sheets 1–10, with explanatory data, CSIRO Australia and Melbourne Univ. Press, Melbourne, Australia.

Owe, M., R. A. M. de Jeu, and T. R. H. Holmes, (2008), Multisensor historical climatology of satellite-derived global land surface moisture, *J. Geophys. Res., 113*, F01002.

Parinussa, R. M., A. G. C. A. Meesters, Y. Y. Liu, W. Dorigo, W. Wagner, and R. A. M. de Jeu, (2011), Error estimates for near-real-time satellite soil moisture as derived from the land parameter retrieval model, *IEEE Geosci. Remote Sens. Lett., 8*, 779–783.

Pipunic, R. C., J. P. Walker, and A. W. Western, (2008), Assimilation of remotely sensed data for improved latent and sensible heat flux prediction: A comparative synthetic study*, Remote Sens. Environ., 112*, 1295–1305.

Pipunic, R. C., J. P. Walker, A. W. Western, and C. M. Trudinger, (2013), Assimilation of multiple data types for improved heat flux prediction: A one-dimensional field study*, Remote Sens. Environ., 136*, 315–329.

Reichle, R. H., R. D. Koster, P. Liu, S. P. P. Mahanama, E. G. Njoku, and M. Owe, (2007), Comparison and assimilation of global soil moisture retrievals from the Advanced Microwave Scanning Radiometer for the Earth Observing System (AMSR-E) and the Scanning Multichannel Microwave Radiometer (SMMR), *J. Geophys. Res., 112*, D09108.

Richter, H., A. W. Western, and F. H. S. Chiew, (2004), The effect of soil and vegetation parameters in the ECMWF land surface scheme, *J. Hydrometeorol.*, *5*, 1131–1146.

Ryu, D., W. T. Crow, X. Zhan, and T. J. Jackson, (2009), Correcting unintended perturbation biases in hydrologic data assimilation, *J. Hydrometeorol.*, *10*, 734–750.

Slater, A. G., and M. P. Clark, (2006), Snow data assimilation via an ensemble Kalman filter, *J. Hydrometeorol.*, *7*, 478–493.

Smith, A. B., J. P. Walker, A. W. Western, R. I. Young, K. M. Ellet, R. C. Pipunic, R. B. Grayson, L. Siriwardena, F. H. S. Chiew, and H. Richter (2012), The Murrumbidgee soil moisture monitoring network data set, *Water Resourc. Res.*, *48*, W07701.

Su, C.-H., D. Ryu, R. I. Young, A. W. Western, and W. Wagner (2013), Inter-comparison of microwave satellite soil moisture retrievals over the Murrumbidgee Basin, southeast Australia, *Remote Sens. Environ., 134*, 1–11.

Turner, M. R. J., J. P. Walker, and P. R. Oke (2008), Ensemble member generation for sequential data assimilation, *Remote Sens. Environ.*, *112*, 1421–1433.

Walker, J. P., G. R. Willgoose, and J. D. Kalma (2001), One-dimensional soil moisture profile retrieval by assimilation of near-surface observations: A comparison of retrieval algorithms, *Adv. Water Resourc., 24*, 631–650.

Whitaker, J. S., and T. M. Hamill (2002), Ensemble data assimilation without perturbed observations, *Monthly Weather Rev., 130*, 1913–1924.

Williams, J., P. J. Ross, and K. L Bristow (1992), Prediction of the Campbell water retention function from texture, structure and organic matter, in *Proceedings of the International Workshop on Indirect Methods for Estimating the Hydraulic Properties of Unsaturated Soils,* edited by M. T. Van Genuchten, F. J. Leij, and L. J. Lund pp. 427–441 Univ. Calif., Riverside, Calif.